Utilization of methanol for polymer electrolyte fuel cells in mobile systems

V.M. Schmidt, P. Bröckerhoff, B. Höhlein, R. Menzer and U. Stimming
Research Centre Jülich (KFA), Institute of Energy Process Engineering, 52425 Jülich (Germany)

Abstract

The constantly growing volume of road traffic requires the introduction of new vehicle propulsion systems with higher efficiency and drastically reduced emission rates. As part of the fuel cell programme of the Research Centre Jülich a vehicle propulsion system with methanol as secondary energy carrier and a polymer electrolyte membrane fuel cell (PEMFC) as the main component for energy conversion is developed. The fuel gas is produced by a heterogeneously catalyzed steam reforming reaction in which methanol is converted to H_2, CO and CO_2. The required energy is provided by the catalytic conversion of methanol for both heating up the system and reforming methanol. The high CO content of the fuel gas requires further processing of the gas or the development of new electrocatalysts for the anode. Various Pt–Ru alloys show promising behaviour as CO-tolerant anodes. The entire fuel cell system is discussed in terms of energy and emission balances. The development of important components is described and experimental results are discussed.

Introduction

The energy consumption in Germany in 1989 shows that approximately one quarter of this energy is consumed by vehicle combustion engines. Road traffic has shown a rising trend for several years characterized by a constant increase in the number of registered cars [1]. Along with the political changes in Germany and Eastern Europe, an increase of the number of cars in Germany from 35.4 million passenger cars in 1990 to 41 or 45.8 million is predicted for the year 2010 [2]. Already today, road traffic contributes more than 47% to the CO, NO_x and C_nH_m emissions as demonstrated in Fig. 1 [3]. Even though the specific emission of the respective pollutant component is limited by law, the further increase of transport requires suitable precautions for emission reduction.

Figure 2 shows a flow chart of various energy conversion sequences discussed for vehicles with different energy carriers and propulsion systems. These sequences are divided into energy production outside the vehicle and storage inside as well as conversion and use of energy in the vehicle. In this paper the potential of methanol as a new energy carrier for a fuel cell-powered vehicle is discussed. In this energy conversion sequence methanol is produced by reforming natural gas followed by synthesis from $H_2/CO_2/CO$. An alternative route can be the use of a non fossil energy carrier, production of hydrogen by electrolysis and production of methanol from H_2/CO_2.

Figure 3 shows the storage volume and weight for different secondary energy carriers as compared with 50 l of gasoline. A comparison of gasoline/diesel, methanol
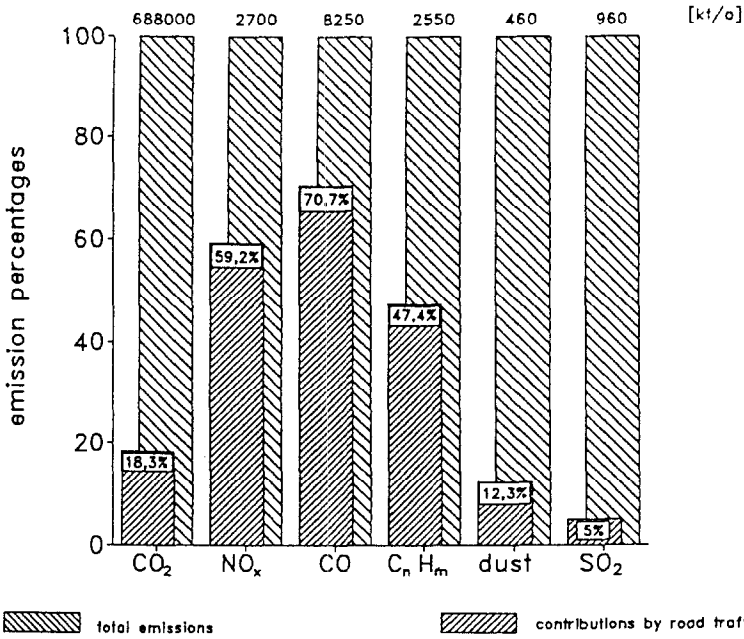
Fig. 1. Total emissions and emissions due to vehicle traffic: CO_2, NO_x, CO, C_nH_m, dust and SO_2 [3].

and hydrogen illustrates that the properties of methanol may be regarded as favourable in comparison with hydrogen.

The utilization of methanol in a fuel cell system for production of electric power could be realized in principle by two different routes. One is the direct electrochemical oxidation of methanol at the anode of a fuel cell. In principle, this is desirable since direct methanol oxidation requires only evaporation of methanol and no reforming. Using platinum as electrocatalyst, however, its activity in oxidizing methanol is smaller by more than two orders of magnitude compared with hydrogen. Thus, the catalytic conversion of methanol to a hydrogen-rich synthesis gas followed by electrochemical oxidation in a H_2/air fuel cell at low temperatures (80 °C) is the process currently preferred. In such a way the advantageous properties of methanol with respect to energy density and storage weight can be combined with the favourable emission-specific properties of electrochemical oxidation of hydrogen. This configuration represents an electrically driven vehicle which has to be compared in terms of energy input and emissions with conventional gasoline and diesel-powered vehicles as well as electric vehicles with a battery for electricity which comes from stationary power plants.

Description of the vehicle propulsion system

The problem associated with road traffic in terms of reducing the quantity and improving the quality of emissions have led to a number of different approaches. The development of hybrid systems for vehicles is one attempt towards solving these problems. An internal combustion engine using gasoline/diesel ensures the required
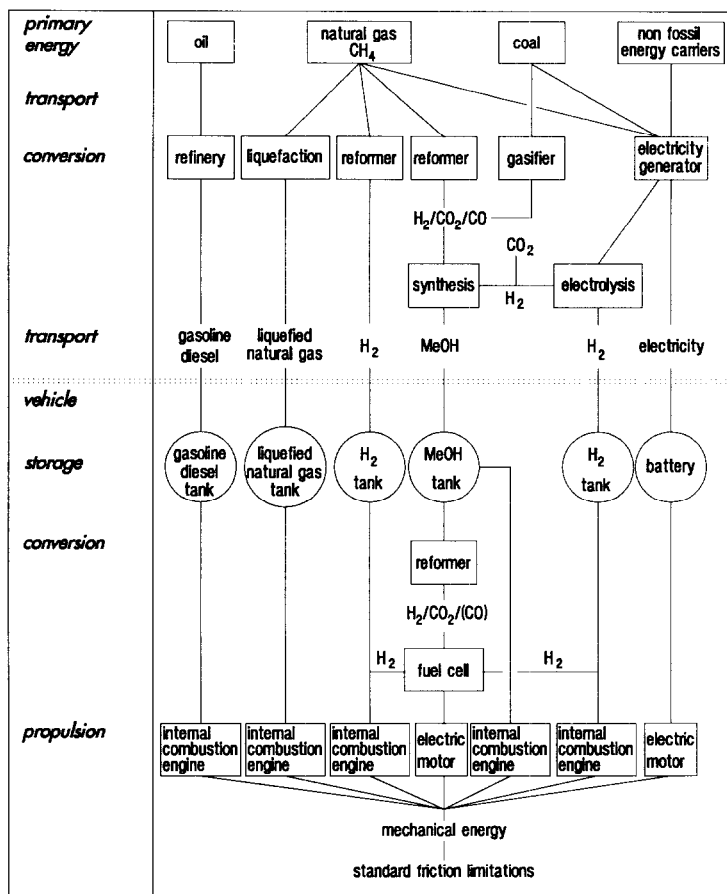
Fig. 2. Flow chart of the energy conversion sequences from primary energy to the wheel for different propulsion systems; the sequence discussed in this paper consists of reforming of natural gas into synthesis gas followed by production of methanol as the secondary energy carrier; in the vehicle, methanol is converted into the fuel gas which is electrochemical oxidized in the fuel cell, the oxidant is air.

range for interurban traffic, while an electric motor is simultaneously available for emission-free operation in urban areas.

When the internal combustion engine in this hybride system is replaced by a methanol reformer connected with a polymer electrolyte fuel cell (PEMFC) the propulsion system, sketched in Fig. 4, is obtained. This concept combines the components of an electric propulsion with the storage potential of a liquid energy carrier. The operating range is limited by the capacity of the methanol tank as in the case of internal combustion engines.

A liquid methanol/water mixture is stored in the tank. A fuel pump delivers the liquid into an evaporator where it is heated, evaporated and superheated. The vapour is then passed into a reformer where a heterogeneously catalyzed reaction takes place reforming methanol/water into a hydrogen-rich synthesis gas (H_2, CO_2, CO). The conversion of the chemical energy of the gas into electric and thermal energy is then

Fig. 3. Storage volume and weight for different energy carriers in comparison with 50 l of gasoline equivalent [3].

Fig. 4. Schematic representation of the propulsion system: methanol reformer, catalytic conversion, PEM fuel cell and electric motor; the electricity from a buffer can be provided by a battery (energy storage) [3].

performed in a PEMFC at temperatures between 80 and 100 °C. This type of fuel cell offers the best possibilities in terms of high power density. Compared with the alkaline fuel cell the solid electrolyte offers better operating conditions and has a high CO_2 tolerance [4, 5]. The PEMFC provides the electric power for the electric motor. The mechanical power of the electric motor is transmitted to the wheels of the car. In addition, electric power can be taken from a battery system previously charged by the fuel cell to cover increased power requirements during acceleration and hill climb.

The start-up phase of the system is carried out by combustion of methanol until all components have reached their operation temperature and full power output. The heat requirement of the reformer during operation is provided by the catalytic combustion of the exhaust gas of the anode side of the fuel cell. The waste heat of the fuel cell can be used to preheat the methanol/water mixture during operation and for air conditioning of the passenger compartment.

Catalytic conversion

Compared with internal combustion engines catalytic conversion processes together with electrochemical conversion provides a large potential for emission reduction. Catalytic combustion represents an alternative to conventional flame combustion in which the high flame temperature (> 1500 °C) produces high amounts of NO_x. The catalytic reaction takes place on a solid catalyst surface at temperatures below the ignition point of methanol (460 °C). The principle of catalytic conversion of chemical into thermal energy is well known since the work of Sir Humphrey Davy (1778–1829); for a detailed discussion see the reviews in refs. 6 to 8.

A test station for the catalytic combustion studies is shown in Fig. 5 [9, 10]. With an estimated value of 22 kW_{el} for the electric power of the fuel cell, the catalytic burner would have to provide a power of about 15 kW. The test station illustrated in Fig. 5 is restricted to 8.8 kW.

The start-up phase using methanol and the combustion of H_2/CO_2 can be simulated. In this case H_2, CO_2 and H_2O amount to 35.1, 45.6, and 19.3% of anode exhaust gas, respectively.

The essential component of the test station is the burner itself. The fuel/air mixture flows in a radial direction through the centre, the top front wall of which is closed by a metal lid. Platinum supported onto Al_2O_3 is used as catalyst which is coated on the outer surface of the ceramic body. The mixture is ignited electrically. Reaction takes place either close to or directly in the catalytic coating. Under experimental conditions power densities up to 50 kW/m^2 with surface temperatures up to 680 °C can be achieved. In this power region combustion is catalytic.

A specific experimental protocol enables the continuous and discontinuous analysis of the combustion products (H_2O, unburnt hydrocarbons (UHC), NO_x, O_2, CO, CO_2, CH_3OH, HCHO and higher aldehydes and ketones). The procedure is described in detail in ref. 11. As the most important result a low CO content in the exhaust gas of about 17 ppm with an air ratio of $\lambda = 1.05$ is obtained. NO_x emission over a wide range of air ratios is less than 0.2 ppm. This can be attributed to the low reaction temperatures resulting from efficient heat extraction.

Reforming of methanol

In a heterogeneously catalyzed reaction methanol/water mixtures can be converted into hydrogen and carbon dioxide:
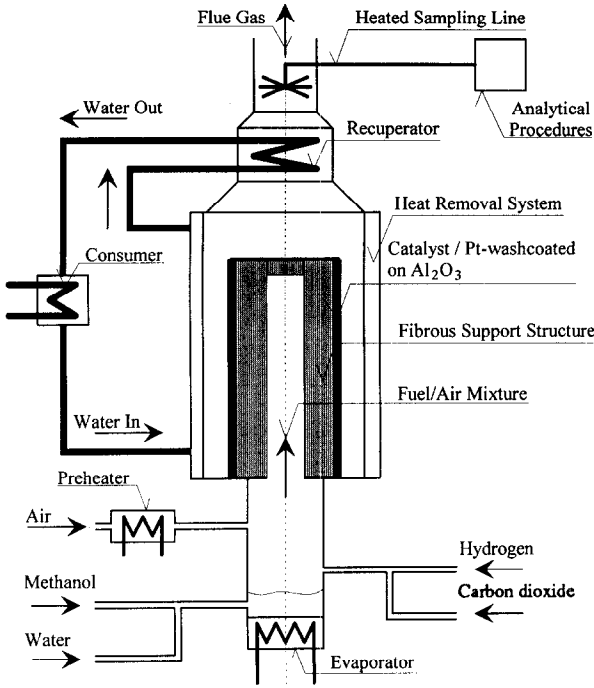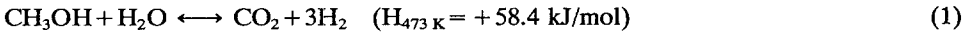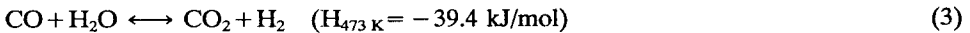
Fig. 5. Schematic diagram of a 8.8 kW catalytic combustion test station.

$$CH_3OH + H_2O \longleftrightarrow CO_2 + 3H_2 \quad (H_{473\,K} = +58.4 \text{ kJ/mol}) \tag{1}$$

In addition, CO is found in the product gas under realistic experimental conditions. According to Hansen and Christiansen [12], the endothermic steam-reforming reaction (1) is accompanied by methanol decomposition:

$$CH_3OH \longleftrightarrow CO + 2H_2 \quad (H_{473\,K} = +97.8 \text{ kJ/mol}) \tag{2}$$

and by the water gas shift reaction:

$$CO + H_2O \longleftrightarrow CO_2 + H_2 \quad (H_{473\,K} = -39.4 \text{ kJ/mol}) \tag{3}$$

It can be shown that, in addition to pressure and temperature, the molar methanol/water ratio has considerable influence on the establishment of the thermodynamic equilibrium. Thermal splitting (eqn. (2)) without adding water leads to a synthesis gas rich in CO (>30%) which is not suitable as a fuel gas for a low-temperature fuel cell. Thus, the CO content in the fuel gas has to be taken into account in the development of a suitable reformer. Even if the CO content can be lowered considerably, CO resistant anodes in the fuel cells are necessary in order to avoid additional components in the periphery. The aspect of a CO tolerant anode will be discussed later (fuel cell section).

The steam reforming of a defined methanol/water mixture permits a reduction of CO in the feed gas in favour of CO_2 and H_2. Figure 6 shows the calculated equilibrium composition of the product gas under given boundary conditions as a function of the water/methanol ratio. At a molar ratio of $n_{H_2O}/n_{CH_3OH} = 1.3$, the equilibrium
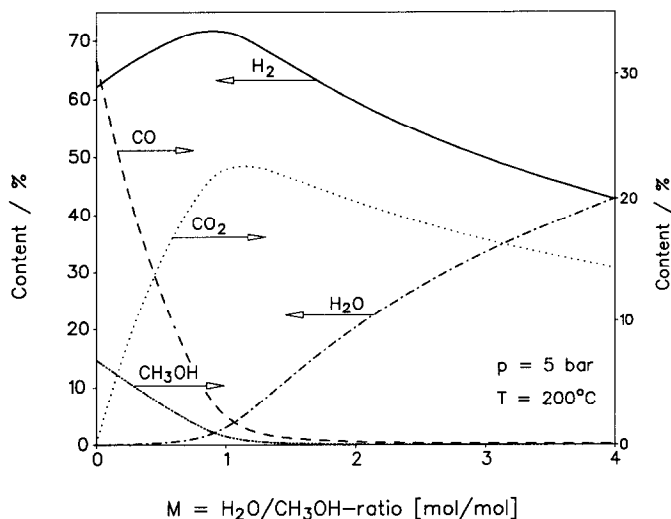
Fig. 6. Composition of the product gas after reforming at the thermodynamic equilibrium as a function of the molar water/methanol ratio [13].

value of the CO content in the dry product gas is about 1 vol.% at $T = 200$ °C and 5 bar [13].

The reforming reaction takes place at temperatures > 150 °C on $CuO/Zn/Al_2O_3$ catalysts using low pressures between 1 and 5 bar. As a consequence, research activities regarding the process engineering of the propulsion system described above have to focus on the optimization of the methanol reformer according to the following criteria:

(i) high hydrogen yield per volume of reformer catalyst and time, e.g., 2–3 m_n^3 H_2/h $dm_{catalyst}^3$ (m_n^3: $T = 0$ °C and $p = 1.01325$ bar);

(ii) high methanol conversion rate of about $> 95\%$;

(iii) low CO content of the synthesis gas of < 1 vol.%, and

(iv) adequate stability of the catalysts under dynamic operating conditions.

In preliminary catalyst tests for an integral methanol reformer under various operating temperatures and with various catalyst loadings under quasi-isothermal operation conditions about 2 to 3 m_n^3 of hydrogen per dm^3 of catalyst/h (methanol conversion $> 95\%$) can be achieved [14]. This optimum hydrogen yield corresponds to a performance of about 6 to 9 kW/dm^3 catalyst and an electric power of 3 to 4.5 kW/dm^3 catalyst which could be realized in a fuel cell with an electric efficiency of about 50%.

Experimental results for a non-isothermally operated integral reformer show a relatively limited operating range for a methanol conversion greater than 95% and a CO content in the synthesis gas of less than 3 vol.%. Simulations also show that the hydrogen production depends on the operating temperature of the catalytic converter [14].

Following the thermodynamic calculations mentioned above, a typical synthesis gas contains about 3% CO, 74% H_2 and 23% CO_2. Further developments of the methanol reformer may require a concept providing for further treatment of the synthesis gas to reduce the fuel gas CO concentration to less than 1 vol.%. This can be achieved by using a second reactor in which the shift reaction (3) could be established at CuO/ZnO catalyst. In this way one additional mole H_2 is produced per mole CO.

Another way of reducing CO in the fuel gas is by methane formation according to:

$$CO + 3H_2 \longleftrightarrow CH_4 + H_2O \quad H_{473\,K} = -214.11 \text{ kJ/mol} \qquad (4)$$
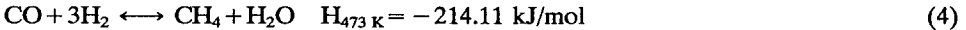
Thermodynamic calculations show that the CO content of the synthesis gas can be reduced to values <1 ppm at reaction temperatures of 20 to 260 °C. Reactors for the shift reaction as well as for methane formation reaction using different catalysts were tested and showed promising behaviour [15].

Finally, it can be concluded that the reduction of the CO content in the fuel gas to a value acceptable for a PEM fuel cell appears a problem which can be solved from a process engineering point of view. It should be noted, however, that additional steps for the fuel gas refinement would lower the total efficiency of the propulsion system.

Polymer electrolyte fuel cell

Two different types of fuel cells are currently being discussed for application in mobile systems: the phosphoric acid fuel cell (PAFC) which operates at temperatures of up to 200 °C using liquid phosphoric acid and the PEMFC with an operating temperature of 60 to 100 °C using a proton-exchange membrane as electrolyte. The PAFC is currently being developed for fuel cell powered buses [16, 17].

Although the PAFC shows a better CO tolerance (<3% of the fuel gas) which is due to the higher operating temperatures, the PEMFC has advantages due to a solid electrolyte, high-power densities and fewer corrosion problems compared with the PAFC. However, as mentioned above, the CO tolerance of the anode in a PEMFC is low. This behaviour is attributed to the fact that the active sites of the Pt catalyst are blocked by adsorbed CO molecules. As an example, for a PEM single cell using H_2 and O_2 at $T = 80$ °C, Lemons [4] reported a decrease in the power density by a factor of two at current densities of 200 mA/cm^2 in the case that the hydrogen gas contains 100 ppm CO.

Under the conditions of using a PEMFC as a component of a propulsion system the further development should concentrate on the following tasks:

(i) high-power densities of up to 1 W/cm^2 of a PEMFC for a small size design of the fuel cell system;

(ii) possibility to operate the fuel cell with synthesis gas containing CO and residual CH_3OH on the anode side and with air on the cathode;

(iii) low catalyst loading at both electrodes;

(iv) minimal energy requirements for supplying the system with air and cooling medium, and

(v) sufficient dynamics of the fuel cell system for the requirements of a vehicle and sufficient long-term stability.

A suitable test station for single PEM fuel cells as well as for cell stacks is illustrated in Fig. 7. In addition, we are able to simulate the operating parameters of a PEMFC with respect to pressure, temperature, flow rate and humidification of the reaction gases, water production and analysis of the exhaust gases. During performance evaluation, the current density is adjusted by a load resistance while the cell voltage is measured by means of a voltmeter. To prevent the drying out of the Nafion® membrane, the reaction gases have to be humidified. Otherwise the ionic conductivity of the solid electrolyte would dramatically decrease. Humidification
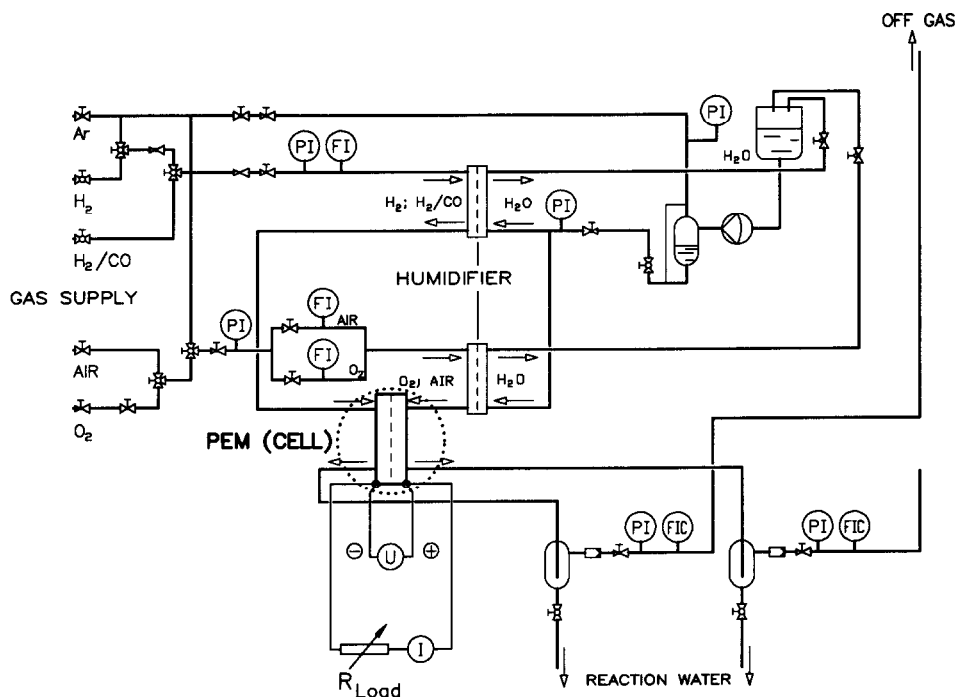
Fig. 7. Schematic representation of the test station for polymer electrolyte fuel cells using H_2 or H_2/CO as anode gas and oxygen/air as cathode gas. PI: pressure indicator, FI: flow indicator, FIC: flow indicator and controller.

(Fig. 7) is performed by two additional single-cell assemblies containing an uncoated Nafion membrane. Water is pressed through the membrane where the gas is saturated with water. In order to get optimal humidification, the humidifier temperature is 15 °C above the fuel cell temperature.

The main components of a single PEM cell obtained from GINER (Waltham, MA, USA) are sketched in Fig. 8. The electrodes are fabricated with carbon-supported Pt black and bonded to a Nafion 117 membrane, where the active electrode area is 40 cm². This membrane electrode assembly (MEA) has titanium screens on both sides between graphite plates which serve as current collectors. Gaskets between the MEA and the graphite plates prevent gas leakage. The overall assembly is held together by two stainless-steel end plates.

First result obtained with this test equipment are shown in Fig. 9 using different H_2/CO gas mixtures. The MEA is a Nafion 117 membrane with integrally bonded TBE® electrode structures (GINER, Inc.). This MEA contains an experimental anode catalyst expecting to have a good tolerance for a hydrogen-containing reformate gas with small quantities of CO. At a current density of 400 mA/cm², a cell voltage of about 0.7 V is measured with pure hydrogen as fuel gas. The CO tolerance of this anode catalyst seems to be acceptable up to 40 ppm CO. At a CO content of 400 ppm, however, the activity of the electrocatalyst is clearly reduced. At such CO contents it is not possible to achieve current densities necessary for an adequate power of the propulsion system.
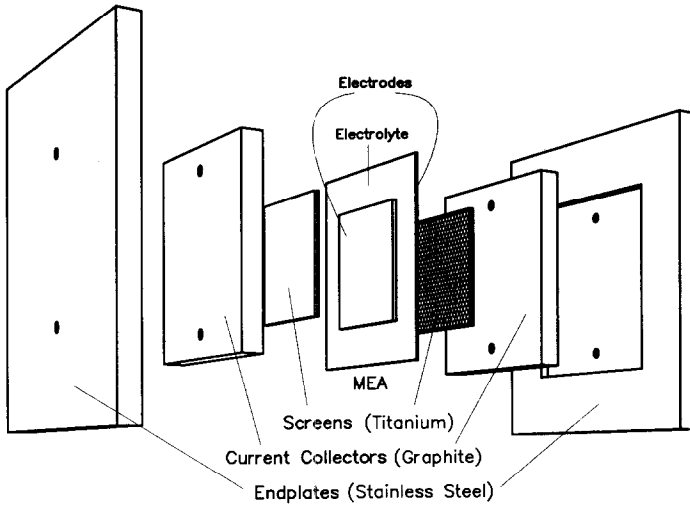
Fig. 8. Schematic of a polymer electrolyte single cell. MEA: membrane electrolyte assembly consisting of Nafion 117® and gas diffusion electrodes; catalyst loading about 4 mg/cm²; electrode area = 40 cm².
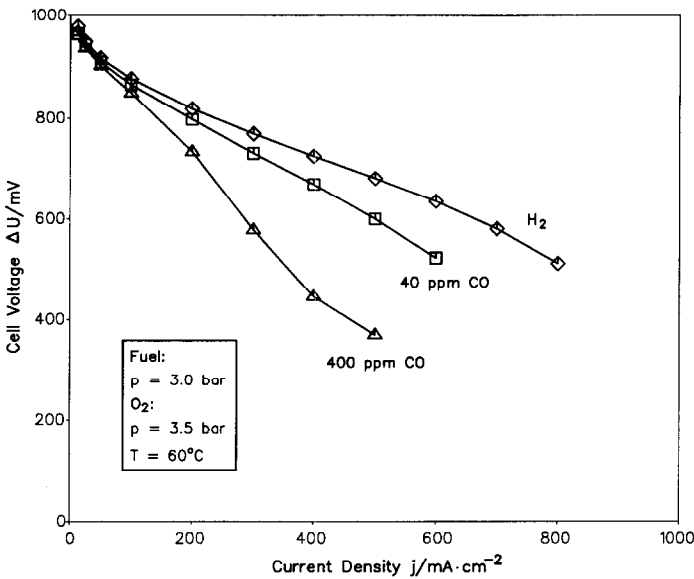

Fig. 9. Cell voltage vs. current density plot for a advanced MEA using different fuel gases at the anode, and pure oxygen at the cathode.

One approach of improving the CO tolerance of the anode is to add small amounts of oxygen (up to 2%) to the hydrogen gas stream which can oxidize CO to a residual value of ≪100 ppm. This was suggested by Gottesfeld [18] and Lemons [4]. This method seems to be very attractive as it would require no additional catalyst or process

steps as described in the previous section. There may be, however, doubts concerning security and difficulties in the process engineering of the fuel cell system due to the fact that the fuel gas would contain oxygen. The direct injection of oxygen could also have long-term damaging effects on the membrane [19].

Another way of possibility solving the CO problem is the development of new electrocatalysts having an enhanced CO tolerance compared with pure platinum. In the literature several bimetallic electrocatalysts based on Pt as the main component were proposed such a Pt–Sn [20–22], Pt–Rh [23] and Pt–Ru [24–26]. These bimetallic electrocatalysts have also shown enhanced electrochemical activity for the direct oxidation of methanol. The surface composition of Pt–Ru alloys in acid media appears to be stable up to potentials of $+1.0$ V versus the reversible hydrogen electrode (RHE) [27]. The enhanced catalytic activity of Pt–Ru towards hydrogen oxidation with H_2/CO gas mixtures can be explained by a promoter effect of Ru. At Ru surface sites the adsorption of water molecules occurs at more negative potentials compared with Pt. As a consequence, CO adsorbed on Pt–Ru (preferentially at Pt sites) can be oxidized to CO_2 at more negative potential possibly according to [24, 25]:

$$Pt-CO + Ru-OH \longrightarrow Pt + Ru + CO_2 + H^+ + e^- \qquad (5)$$
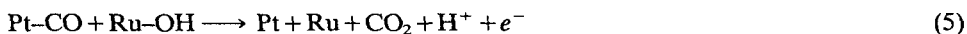
As a model system Pt–Ru alloys were chosen which had a defined bulk as well as surface composition which were determined by means of atomic absorption spectroscopy, X-ray diffraction and neutral secondary mass spectrometry. Furthermore, the CO adsorption on pure Pt and Pt–Ru alloys was studied by means of Fourier-transform infrared spectroscopy (FT–IR) [28]. The enhanced activity of Pt–Ru in comparison with Pt can be demonstrated in Fig. 10. The potential for CO adsorbate oxidation is shifted to negative potentials in the case of Pt–Ru. The FT–IR data show that the CO coverage is lower on Pt–Ru and the peak potential for CO adsorbate oxidation is shifted by about 200 mV to lower potentials.

These results obtained on smooth Pt–Ru electrodes were applied to real fuel cell gas diffusion electrodes with a defined Pt–Ru ratio. Pt–Ru with an average particle diameter of 3 to 6 nm was deposited onto carbon supports. Figure 11 shows preliminary results for a MEA with low Pt–Ru loadings of about 0.5 mg alloy/cm^2 on Vulcan XC 72 (ElectroChem, Woburn, MA, USA) as the anode. This was compared with the corresponding gas-diffusion electrodes but with pure Pt as catalyst. The catalyst loading was the same for both anodes. The cathode material for both MEAs was identical and consisted of Pt dispersed on Vulcan XC 72. The cell voltage versus time plots for both cells operating at the same current density demonstrate that the poisoning effect on dispersed Pt–Ru is lower than on dispersed Pt. However, the performance of such MEAs have yet to be improved towards higher power densities.

Energy and emission balance

In order to obtain the energy balance of the complete propulsion system consisting of methanol reformer, PEMFC and catalytic conversion, it is assumed that the efficiency of the PEMFC is 50% (based on lower heating value) and the methanol conversion is >95% in the reformer unit. Assuming a passenger car with 22 kW$_{el}$ power of the electric motor the fuel cell requires a methanol flow of 52.5 kW which corresponds to a consumption of 12 l methanol per hour. In addition, 22 kW are waste heat with a temperature level of about 100 °C and other power losses amounting to 8.5 kW; 25% of the energy of the hydrogen-rich product gas of the reformer is converted into low-temperature heat in the catalytic conversion with favourable emissions. The energy

310
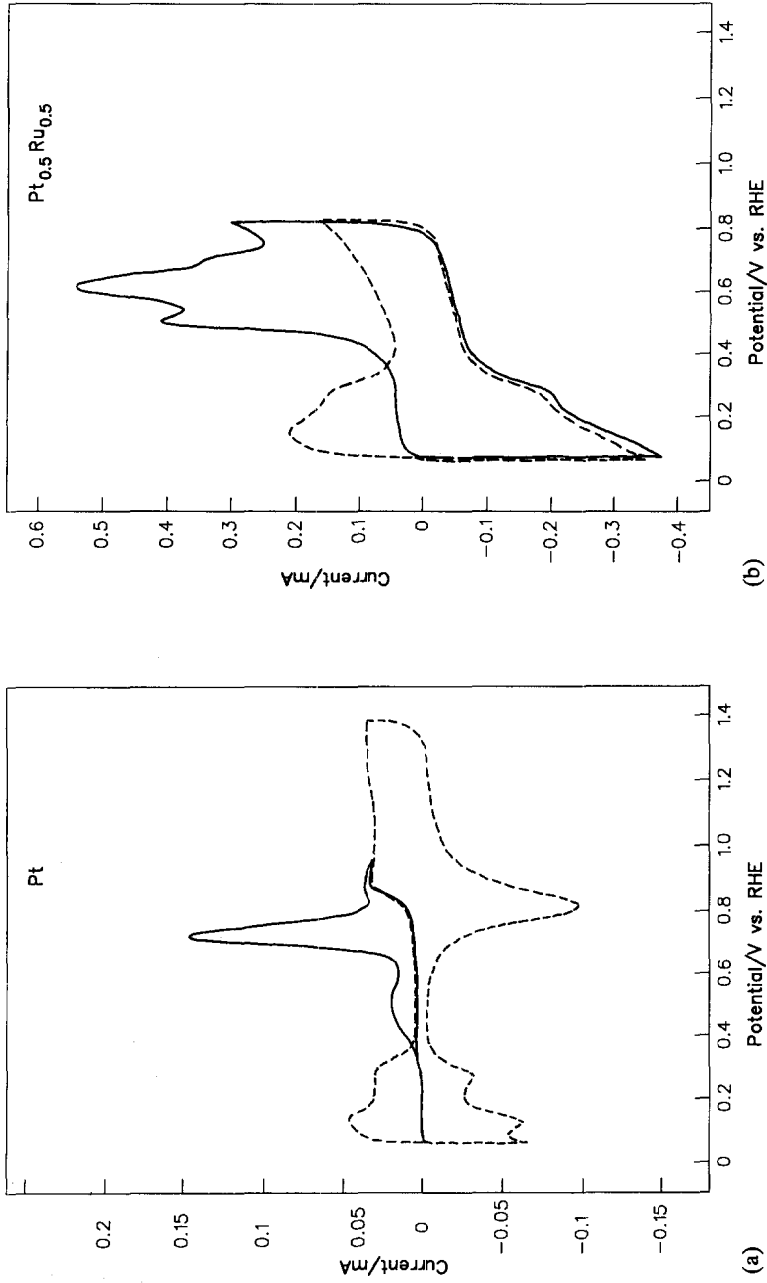
Fig. 10. Potentiodynamic profile of the oxidation of CO adsorbed on (a) polycrystalline Pt and (b) $Pt_{0.5}Ru_{0.5}$ electrodes in 1 M $HClO_4$ (dashed line: supporting electrolyte). Atomic ratio of Pt:Ru=50:50; adsorption potential of CO=100 mV vs. RHE; sweep rate: 20 mV/s, and geometric electrode area=0.78 cm^2.
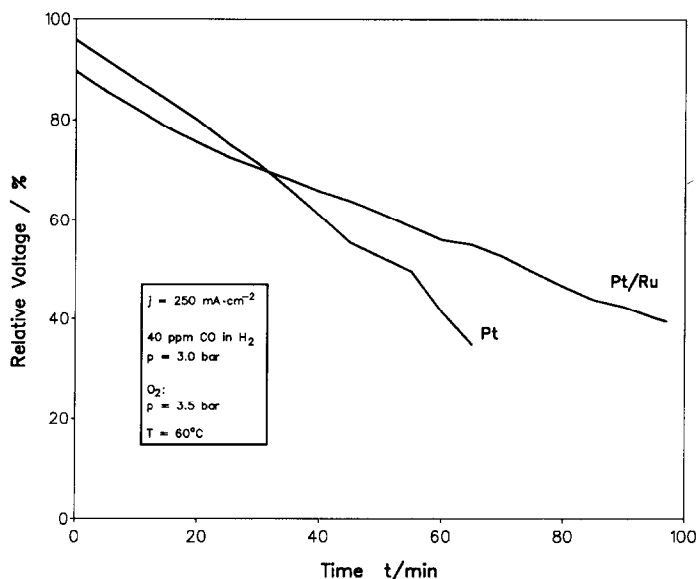
Fig. 11. Relative cell voltage vs. time plot for two different MEAs with highly dispersed Pt and Pt–Ru (atomic ratio: 50:50) on Vulcan XC 72 as anode material (catalyst loading: 0.5 mg/cm^2). Fuel gas at the anode is hydrogen containing 40 ppm CO, oxygen at the cathode; initial cell voltage 470 mV at a constant current density of j = 250 mA/cm^2, and the 100% value corresponds to pure hydrogen as fuel gas.

produced by catalytic conversion covers the heat requirements of the reformer for heating, evaporation, reforming and superheating.

The limited dynamics of the methanol reformer during operation conditions can be compensated using a battery system. In a parallel hybrid propulsion mode the electric motor can be simultaneously powered by the system reformer/fuel cell and the battery. In this way the different time constants during startup phase, acceleration and peak power requirements can be satisfied. The range is limited by the capacity of the methanol tank and no energy losses due to external battery charging and discharging arise.

The specific energy consumption and corresponding CO$_2$ emission depend on the final concept of the components of such a fuel cell vehicle. Using reasonable assumptions, it will be considerably lower than that of a gasoline-powered internal combustion engine [29]. In addition, the emissions of NO$_x$, CO, and C$_n$H$_m$ using methanol in the fuel cell propulsion system are considerably lower [3].

Summary and outlook

The presented concept of a vehicle propulsion system with methanol as the secondary energy carrier and hydrogen as the fuel gas for a low-temperature fuel cell combine the favourable properties of a liquid form of energy with the specific emission advantages of hydrogen. This configuration provides a propulsion system with clear advantages compared with conventional systems.

In a heterogeneously catalyzed reforming reaction, methanol is converted into a hydrogen-rich fuel gas which contains CO and CO_2. The energy for the startup phase and for the reforming reaction is produced using the catalytic combustion of methanol at Pt surfaces at temperatures below the ignition point of methanol. As a consequence, CO and NO_x emissions are low compared with direct combustion. A polymer electrolyte fuel cell which operates at temperatures of 60 to 80 °C produces the power necessary for the electric motor of the vehicle. This fuel cell type offers a high power density and a compact design suitable for vehicle propulsion. Nevertheless, the CO content of the fuel gas requires the development of new electrocatalysts for the anode or an almost complete removal of CO from the fuel gas.

Although the propulsion system described in this paper consist of a complex arrangement of components, their optimized connection promises an emission balance which can result in reducing the quantity, especially of NO_x, CO and C_nH_m by orders of magnitude.

References

1 Der Bundesminister für Verkehr (ed.), *Verkehr in Zahlen 1991*, Vol. 20, 1991.
2 German Shell AG, Motorisierung nach der Vereinigung: Aufbruch zu neuen Dimensionen, *Aktuel. Wirtschaftsanalysen, 9* (No. 22) (1991).
3 B. Ganser, B. Höhlein and C.B. von der Decken, *VDI Ber., 1020* (1992) 341.
4 R.A. Lemons, *J. Power Sources, 29* (1990) 251.
5 S. Srinivasan, D.J. Manko, H. Koch, M.A. Enayetullah and A.J. Appleby, *J. Power Sources, 29* (1990) 367.
6 D.L. Trimm, *Appl. Catal., 7* (1983) 249.
7 R. Prasad, *Catal. Rev.–Sci. Eng., 26* (1984) 1.
8 L.D. Pfefferle and W.C. Pfefferle, *Catal. Rev.–Sci. Eng., 29* (1987) 219.
9 P. Bröckerhoff and B. Emonts, in A. Holmes, K.-J. Jens and S. Kolboe (eds.), *Natural Gas Conversion*, Elsevier, Amsterdam, 1991, p. 557.
10 P. Bröckerhoff and B. Emonts, *Brennst.-Wärme-Kraft, 42* (1990) 514.
11 E. Emonts, *Dissertation D 82*, Technical University, Aachen, Research Centre Jülich (Jül-2275), 1989.
12 J.B. Hansen and H. Christiansen, in J.B. Goodenough and J. Jemsem (eds.), *Solid State Protonic Conductors 2*, University Press, Odense, 1983, pp. 335–345.
13 B. Ganser and B. Höhlein, *Proc. 9th World Hydrogen Energy Conf., Paris, France, June 22–25, 1992*, p. 1321.
14 B. Ganser, *Dissertation D 82*, Technical University, Aachen, Research Centre Jülich (Jül-2748), 1993.
15 G. Colsmann, *Diploma Thesis*, Technical University, Aachen, 1992.
16 R. Kevala, *Ext. Abstr., Fuel Cell Seiminar, Tucson, AZ, USA, Nov. 29–Dec. 2, 1992*, p. 41.
17 O. Yamamoto, H. Tajima and S. Ohga, *Ext. Abstr., Fuel Cell Seminar, Tucson, AZ, USA, Nov. 29–Dec. 2, 1992*, p. 46.
18 G. Gottesfeld and J. Pafford, *J. Electrochem. Soc., 135* (1988) 2651.
19 J.C. Amphlett, K.A.M. Creber, J.M. Davis, R.F. Mann, B.A. Peppley and D.M. Stockes, *Proc. 9th World Hydrogen Energy Conf., Paris, France, June 22–25, 1992*, p. 1541.
20 K.J. Cathro, *J. Electorchem. Soc., 116* (1969) 1608.
21 M.M. Janssen and J. Moolhuysen, *Electrochim. Acta, 21* (1976) 861.
22 S.R. Wang and P.S. Fedkiw, *J. Electrochem. Soc., 139* (1992) 3151.
23 P.N. Ross, K. Kinoshita, A.J. Scarpellino and P. Stonehart, *J. Electroanal. Chem., 59* (1975) 177.
24 M. Watanabe and S. Motoo, *J. Electroanal. Chem., 60* (1975) 267.
25 P.N. Ross, K. Kinoshita, A.J. Scarpellino and P. Stonehart, *J. Electroanal. Chem., 63* (1975) 97.

26 K. Franaszczuk and J. Sobkowski, *J. Electroanal. Chem.*, *327* (1992) 235.
27 E. Ticianelli, J.G. Beery, M.T. Paffett and S. Gottesfeld, *J. Electroanal. Chem.*, *258* (1989) 61.
28 R. Ianiello, V.M. Schmidt, U. Stimming, J. Stumper and A. Wallau, *Process in Electrocatalysis: Theory and Practice, Ferrara, Italy, Sept. 12–15, 1993.*
29 S. Birkle, R. Kircher, C. Nölscher, H. Voigt, B. Ganser and B. Höhlein, in preparation.